



Study and sizing of a multi-source pumping system

Karim Amrouche *, Radia Abdelli, Naser-Eddine Benhacine

Université de Bejaia, Faculté de Technologie, Laboratoire de Technologie Industriel et de l'Information (LTII), Algérie.

ARTICLE INFO

Article history:

Received April 16, 2024

Accepted April 22, 2024

Keywords:

Photovoltaic system

Wind power system

Battery

Pumping

Sizing

Energy management

ABSTRACT

The growth of renewable energy development and exploitation has been strong in recent years. The multisource pumping is considered as one of the most widely adopted solutions in rural (agricultural) areas. This paper presents a study of different components of the system, including both photovoltaic and wind generators with MPPT, batteries, and a motor-pump unit. It further explores sizing and energy management. The process of sizing involves determining the optimal component capacities to meet energy demands, taking into account variables such as energy source variability and load profiles. In parallel, energy management strategies are critical to balance energy supply and demand, mitigate intermittency issues, and extend the lifespan of energy storage components. This paper explores the sizing and energy management of a multi-source system comprising a photovoltaic generator, a wind turbine with MPPT methods, a battery storage, and a motor pump to meet power requirements.

1. INTRODUCTION

Our planet is being impacted by the excessive use of fossil fuels, and these finite resources are also set to dry up in the coming years. Energy and water scarcity pose significant challenges for numerous residents living in the rural and remote regions of developing countries. The issue of limited water resources in these distant areas is of paramount importance to the local populations. The pursuit of suitable remedies for this problem plays a vital role in enhancing living standards in such regions. Hybrid system pumping emerges as the perfect solution for providing water supply in these remote and rural locations. (Xiao Xu, 2020) (Obaid W, 2021)

A hybrid system with storage is proposed to reduce the overheating of the motor temperature and increase efficiency. The storage serves as both an energy reservoir for surplus power and a backup energy source (Serir Ch, 2016). To guarantee the efficient and dependable performance of a hybrid system, it is imperative to coordinate and optimize the energy sources employed within the system. This

* Corresponding author, E-mail address: karim.amrouche@univ-bejaia.dz



action is achieved through the implementation of energy management algorithms, several researches have been conducted on the subject. (Gam O, 2019) (Zaibi M, 2018) (Poompavai T, 2019)

In this paper, we introduce a hybrid pumping system powered by solar and wind sources with battery storage. The system also incorporates an induction motor controlled through rotor flux-oriented vector control. This motor is linked to a centrifugal pump, which is coupled with a strategically placed elevated water storage tank. To maximize power extraction from both the photovoltaic panel and the wind turbine, we have employed two distinct Maximum Power Point Tracking (MPPT) techniques, the P&O for the photovoltaic and the classical for the wind turbine. Furthermore, we have integrated the necessary power converters to ensure the system's proper functionality. To guarantee efficient management of the available energy and meet power demands, we have carried out system sizing and developed an energy control and management algorithm.

We have presented the necessary steps for the sizing of a hybrid pumping system combining photovoltaic and wind sources with batteries, along with a strategically positioned water tank for a site located in a rural region. This system is designed to provide the required energy to power the load, and also ensure a reliable water supply for the region's needs. A power management algorithm has been presented to ensure energy availability and proper operation throughout the year. After a simulation on MATLAB/Simulink, the obtained results show the efficiency and reliability of the proposed system.

2. Description of the system

Figure 1 shows a block diagram of the proposed system

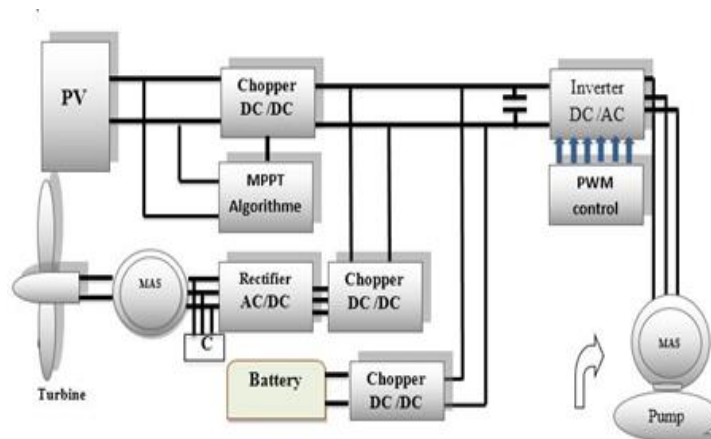


Fig 1. Proposed system scheme

The system includes PV Panels, a DC/DC converter with MPPT control, a wind turbine with MPPT control, an induction motor, a three-phase PWM inverter, a centrifugal pump, and a battery.

3. MODELING SYSTEM

3.1 Photovoltaic generator

This model is characterized by a very simple resolution. It requires only four parameters namely I_{sc} , V_{oc} , I_m , and V_m . The (I_{pv}, V_{pv}) characteristic of this model is illustrated as follows (Serir Ch, 2016) (Pant S, 2020):

$$I_{pv} = I_{sc} \left[1 - C_1 \left(\exp \left(\frac{V_{pv}}{C_2 V_{oc}} \right) - 1 \right) \right] \quad (1)$$

$$\text{With: } \begin{cases} C_1 = I_{sc} \left[1 - \left(\frac{I_m}{I_{sc}} \right) \right] e^{-\frac{V_m}{C_2 V_{oc}}} \\ C_2 = \frac{\left(\frac{V_m}{V_{oc}} \right) - 1}{\ln \left(1 - \frac{I_m}{I_{sc}} \right)} \end{cases} \quad (2)$$

3.2 Turbine

The optimal wind turbine power (with MPPT) versus time PWT(t) has the following expression (Zaibi M, 2018):

$$P_{WT}(t) = \frac{1}{2} \eta_{sc} \eta_g C_{p,opt} \rho A_{WT} V_{wind}^3(t) \quad (3)$$

With:

- η_{sc}, η_g static converter efficiency, generator efficiency,
- $C_{p,opt}$ optimal wind turbine power coefficient (i.e. corresponding to a perfect maximum point tracker),
- ρ air density (kg/m^3),
- A_{WT} wind turbine swept area (m^2),
- $V_{wind}(t)$ wind speed versus time (m/s).

3.3 CIEMAT battery model

The battery's model is characterized by the series connection of an electromotive force with a variable resistance, as follows (Laadissi1 E.M, 2018):

$$V_{bat} = n_b \cdot E_b \pm n_b \cdot R_b \cdot I_{bat} \quad (4)$$

With: n_b is cell number, V_{batt} : battery voltage, I_{batt} : battery current, E_{batt} : electromotive force.

3.4 Induction Machine

The electric equations of the induction machine are written in matrix form as follows (Chouidira I, 2020):

$$\begin{bmatrix} v_{ds} \\ v_{qs} \\ 0 \\ 0 \end{bmatrix} = \begin{bmatrix} R_s & -\omega_s l_s & 0 & -\omega_s \cdot L_m \\ \omega_s l_s & R_s & \omega_s \cdot L_m & 0 \\ -R_r & \omega_r \cdot l_s & R_r & -\omega_r (l_r + L_m) \\ -\omega_r \cdot l_r - R_r & -\omega_r (l_r + L_m) & R_r & \end{bmatrix} \cdot \begin{bmatrix} i_{sd} \\ i_{sq} \\ i_{md} \\ i_{mq} \end{bmatrix} + \begin{bmatrix} l_s & 0 & L_{md} & L_{dq} \\ 0 & l_s & L_{dq} & L_{mq} \\ -l_r & 0 & L_r & 0 \\ 0 & -l_r & L_{dq} & l_r + L_{mq} \end{bmatrix} \cdot \begin{bmatrix} \frac{di_{sd}}{dt} \\ \frac{di_s}{dt} \\ \frac{di_{md}}{dt} \\ \frac{di_{mq}}{dt} \end{bmatrix} \quad (5)$$

The expression of the electromagnetic torque is:

$$T_{em} = P \cdot L_m \cdot (i_{md} \cdot i_{sq} - i_{mq} \cdot i_{sd}) \quad (6)$$

3.4 Centrifugal pump

The head-Flowrate $h - Q$ characteristic can be expressed approximately by the following Quadratic form: (Goppelt F, 2018)

$$H = a_0 \omega^2 - a_1 \omega Q - a_2 Q^2 \quad (7)$$

Where a_0 , a_1 , and a_2 are the coefficients generally given by the manufacturers. The hydraulic power, resistive torque, and mechanic power are given by: (Perissinotto R M, 2021)

$$P_H = \rho g Q H, \quad T_r = k_r \omega^2 + C_s \quad (8), (9)$$

The pump efficiency is defined as the ratio of the hydraulic power imparted by the Pump to the fluid to the shaft mechanical power and is given by:

$$\eta_p = \frac{\rho_H g H Q}{C \left(1 - \frac{\omega_{s1}}{\omega_s}\right)^3 \omega_s} \quad (10)$$

where Q , H , ρ , g , ω_s , and ω_{s1} are the water flow (m^3/s), the total height of the well (m), the density (Kg/m^2), and the gravity (m/s^2), the angular frequency of the supply (rad/s) and the slip speed (rad/s), respectively.

3.5 Flux-Oriented Vector Control of the Squirrel Cage Induction Machine

The motor's equations with the constraint $\phi_{qs} = 0$ et $\phi_{dr} = \phi_r$ is simplified as follows:

$$\left\{ \begin{array}{l} V_{rd} = \sigma L_s \frac{di_{sd}}{dt} + \left(R_s + \frac{M^2}{L_r^2} R_r \right) i_{sd} - \sigma L_s \omega_s i_{sq} - \frac{M R_r}{L_r^2} \phi_r \\ V_{rd} = \sigma L_s \frac{di_{sq}}{dt} + \left(R_s + \frac{M^2}{L_r^2} R_r \right) i_{sq} + \sigma L_s \omega_s i_{sd} + \frac{M_r}{L_r^2} \omega \phi_r \\ \frac{d\phi_r}{dt} = \frac{M}{T_r} i_{sd} - \frac{1}{T_r} \phi_r \\ \omega_r = \frac{M i_{sq}}{T_r \phi_r} \\ P_{em} = \frac{T_{em} \omega_s}{p} \\ T_{em} = \frac{PM}{L_r} \phi_r i_{sq} \end{array} \right. \quad (11)$$

4. SIZING AND MANAGEMENT

4.1 Pumping system sizing

We will take the photovoltaic generator as the main source, the wind system as a complementary source, batteries for compensation, and a water tank to meet the water needs of a small village containing 170 families. From what we need to make a sizing of the various components of the studied system. The daily consumption of the village is therefore estimated at 72.25 m³ so we will take a tank of 110 m³, the dynamic level head is about 12 m and the nominal flow rate is 25 m³/h. The results obtained from the sizing system are presented in Table 1.

Table 1. Sizing pumping system

Symbols	Expressions	Results
Hydraulic power	$P_{hyd} = \rho g Q H$	817.5 W
Mechanical power required by the pump	$P_{mec} = \frac{P_{hyd}}{\eta_p}$	1486.36 W
Electric power	$P_{ele} = \frac{P_{mec}}{\eta_{lm}}$	1748.66 W
Input power of the inverter	$P_{dem} = \frac{P_{ele}}{\eta_{inv}}$	1840.69 W
Necessary pumping time	$\tau_p = \frac{V}{Q}$	4.4 h
Daily electrical energy required by the load	$E_c = P_{dem} \tau_p$	8099.036 Wh/day
The power of the PV generator	$P_{PV} = \frac{E_{ele}}{\tau_p (1 - pertes)}$	2300.8625 W
Number de panels	$N_{PV} = \frac{P_{PVt}}{P_{PV}}$	21 panels
Number of panels series	$N_{PVs} = \frac{V_{dc}(1 - \alpha)}{V_m}$	7 panels
Number of panels parallel	$N_{PVp} = \frac{\frac{P_{PV}}{V_{dc}(1 - \alpha)}}{I_m}$	3 panels
Battery capacity	$C_{bat} = \frac{E_c N_{jaut}}{V_{bat} PDDR_{bb} N_m}$	150 A.h

With: N_{jaut} : number of days of autonomy, PDD: depth of discharge, R_{bb} : battery performance, N_m : number of days in the month.

Speed reference of motor-pump: The reference speed (ω_{ref}) is determined by the total power (photovoltaic, wind, and batteries) and is given by the following relation:

$$\omega_{\text{ref}} = \omega_n \times \sqrt[3]{\frac{P_{\text{tot}} \times \eta}{P_n}} \tag{12}$$

With:

- ω_{ref} : Rated speed of the asynchronous machine [rad/s].
- P_{tot} : Total power (photovoltaic, wind, and batteries) [W].
- η : Efficiency of the motor-pump unit.
- P_n : Rated power of the motor [W]

After sizing, we need 21 panels of 120 Wc (7 in series and 3 in parallel) as the main generator, while the 1KW wind system will be a complementary generator, and 6 batteries will be used for compensation.

4.2 Supervisor control

To maintain a reliable water supply, the entire system must operate perfectly and effectively. Achieving this goal requires the optimal management of energy flow between different components. The management system plays a critical role in overseeing energy transfers among these components and in regulating the charging and discharging processes of the storage (batteries) to extend their lifespan.

From this management system, we can establish five modes of operation, which are summarized in Table 2:

Table 2. Management system

Mode	Description	Action
1	Hybrid Power = Load Demand	Disconnect the battery, and direct supply to the load.
2	Hybrid Power > Load Demand, SOC < SOCmax	Supply the load and charge the battery.
3	Hybrid Power > Load Demand, SOC > SOCmax	Disconnect the battery. The load is powered by both generators; excess energy goes to the load-dumping resistor.
4	Hybrid Power < Load Demand, SOC > SOCmin	Battery compensates for power deficit.
5	Hybrid Power < Load Demand, SOC < SOCmin	Disconnect both battery and load.

Figure 2 represents the energy management algorithm:

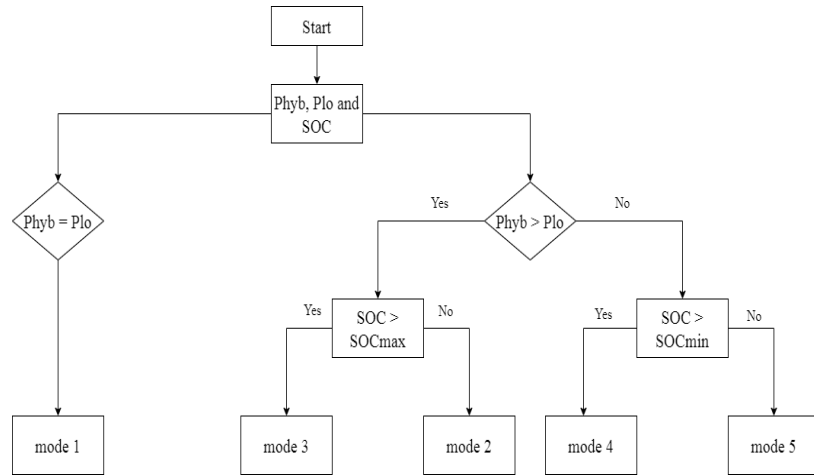


Fig 2. Proposed flowchart

4. SIMULATION RESULTS

Utilizing the previously described models and control methods, a simulation of a multisource pumping system has been developed and conducted within the MATLAB/Simulink environment.

Irradiation, temperature, and wind speed exhibited daily variations over 12 days in October. These variations are quantified by the average values for each parameter per day, and they are visually depicted in Figure 2, Figure 3, and Figure 4. Figure 5 represents the powers (P_{hyb} , P_{bat}), while it is noted that the hybrid power and that of the battery (charge and discharge) are complementary.

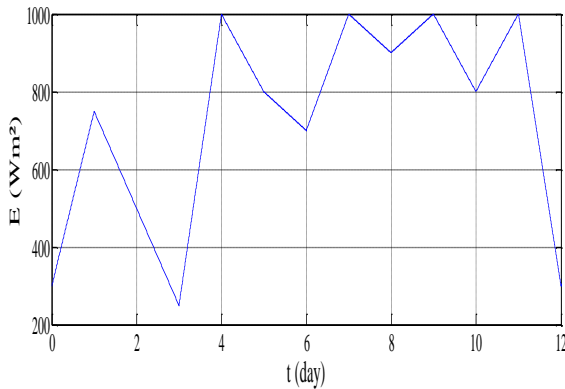


Fig 2. Solar irradiance

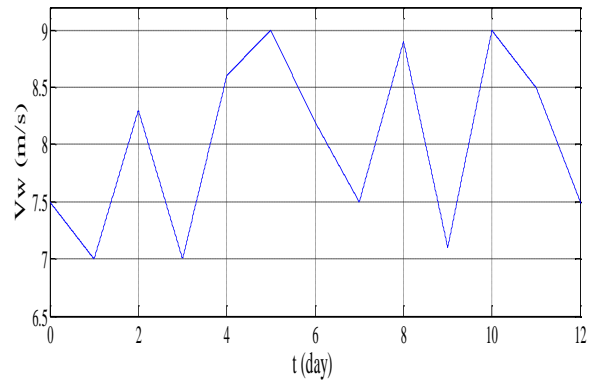


Fig 3. Wind speed

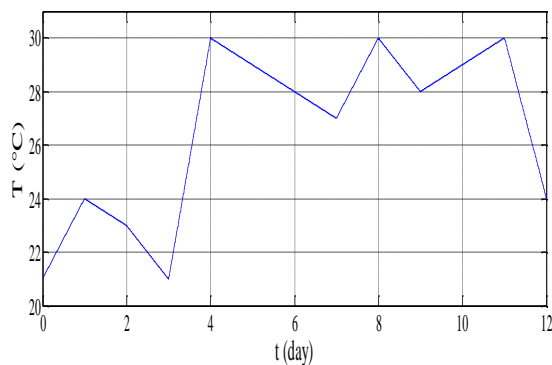


Fig 4. Ambient temperature

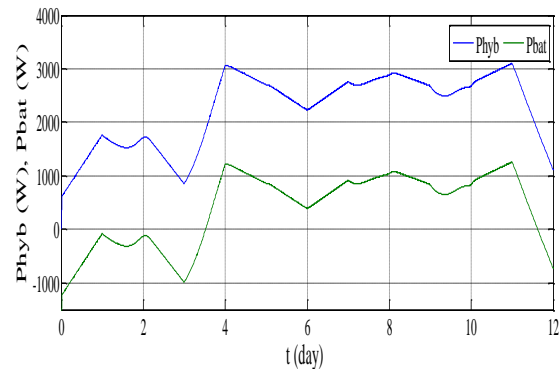


Fig 5. Hybrid and battery power

After management, Figure 6 shows that the powers (hybrid, battery) are complementary. At moments (0 to 3.5), and (11.5 to 12), the battery compensates for the power deficit to supply the load ($P_{\text{hyb}} < P_{\text{lo}}$). In this case, the battery acts as a source. At the moment (3.5 to 11.5), the hybrid power is greater than or equal to the power demanded ($P_{\text{hyb}} \geq P_{\text{lo}}$), here the battery disconnects and does not contribute, and the excess energy is used to charge the battery.

Water flow is almost constant as shown in Figure 7 which means the availability of energy at all times.

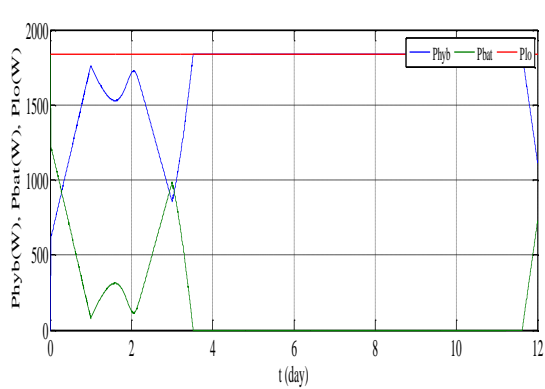


Fig 6. Hybrid, battery and load power after management

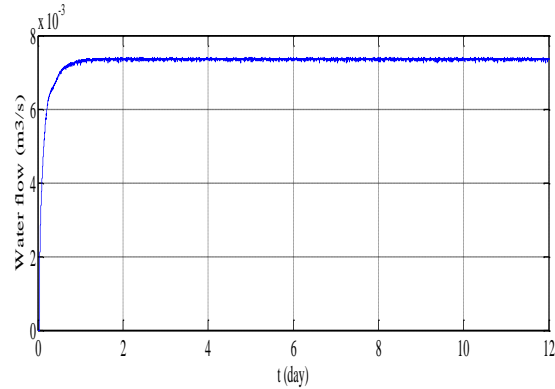


Fig 7. Water flow

It can be observed that the estimated speed evolves until it reaches the reference speed value in Figure 8, and the rotor flux increases slowly until it stabilizes at its reference value of 0.7 Wb in Figure 9.

The electromagnetic torque and the resistive torque are nearly equal, for each value of the resistive torque, the electromagnetic torque tends to track the value imposed in Figure 10, the direct and quadrature currents in Figure 11 and Figure 12 closely track their references, and the stator current in figure 13 and figure 14 are sinusoidal.

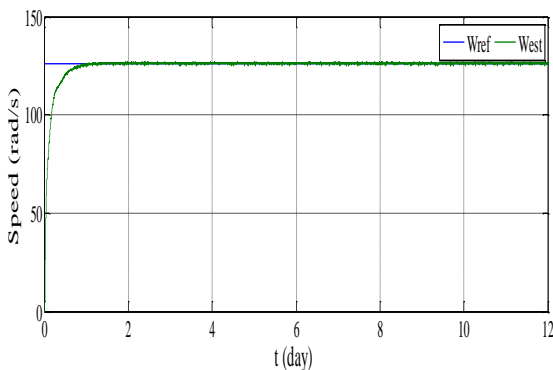


Fig 8. Reference and estimated speed

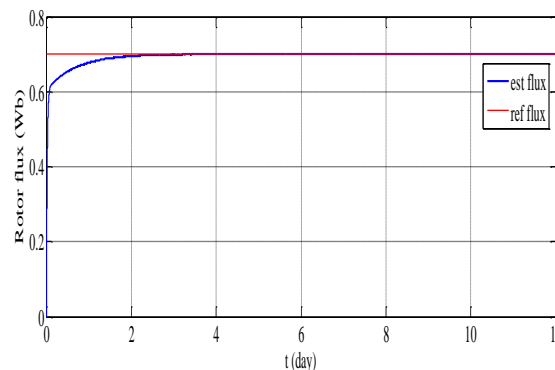


Fig 9. Rotor flux

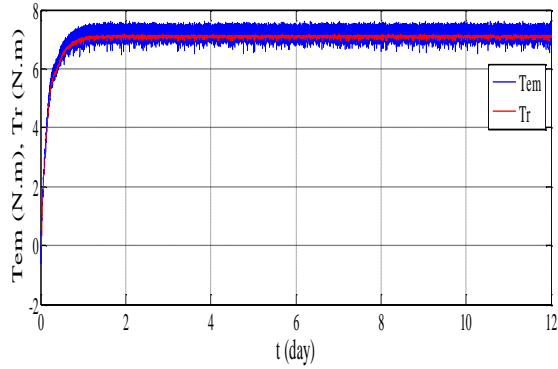


Fig 10. Electromagnetic and resistive torque

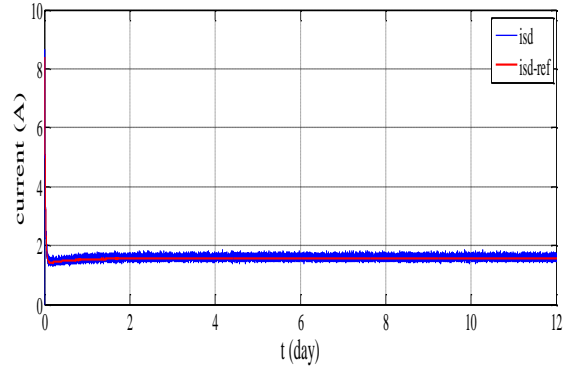


Fig 11. Currents waveform isd-ref, isd

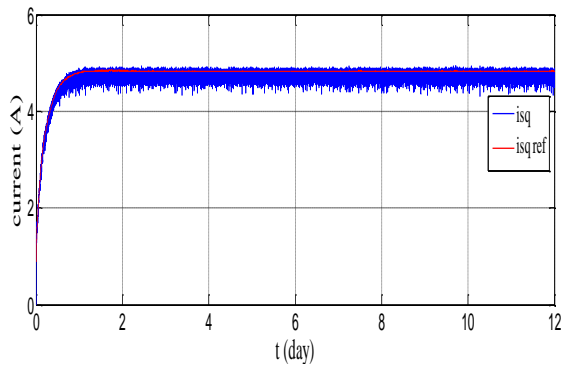


Fig 12. Current waveform isq_ref, isq

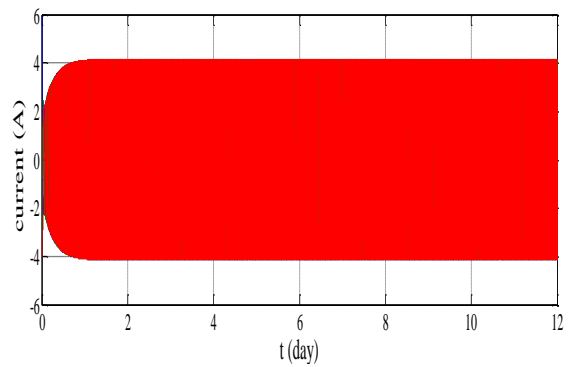


Fig 13. The waveform of the stator current

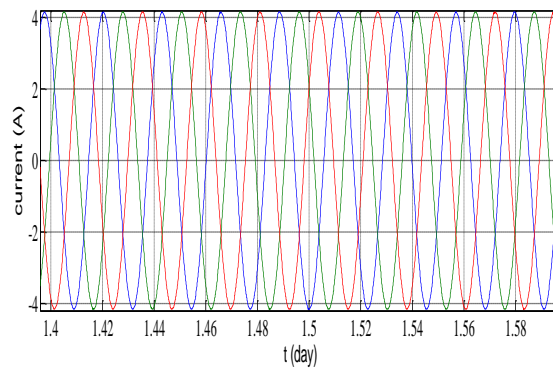


Fig 14. Zoom of the waveform of the stator current

5. CONCLUSION

We have presented the necessary steps for the sizing of a multisource pumping system combining photovoltaic and wind sources with batteries, along with a strategically positioned water tank for a site located in a rural region. This system is designed to provide the required energy to power the load, and also ensure a reliable water supply for the region's needs. A power management algorithm has been presented to ensure energy availability and proper operation throughout the year. After a simulation on MATLAB/Simulink. The obtained results show the efficiency and reliability of the proposed system.

APPENDIX

Parameters of the wind turbine, the asynchronous generator, the photovoltaic panel, and the asynchronous motor

Table 3. Parameters of wind turbine

Rated power	1000 W
Blades	3
Blades diameters	2.26 m
Startup wind speed	3.4 m/s
Rated wind speed	12.5 m/s

Table 4. Parameters of the asynchronous generator

Stator resistance	5.75 Ω
Roto resistance	4.2 Ω
Stator inductance	0.4662 H
Rotor inductance	0.4662 H

Table 5. Parameters of the photovoltaic panel

Maximum power	110 W
Rated current	3.15 A
Rated voltage	35 V
Short-circuit current	3.45 A
Open circuit voltage	43.5 V
Temperature coefficient of I_{sc}	1.4 mA/ $^{\circ}C$
Temperature coefficient of V_{oc}	-152 mA/ $^{\circ}C$

Table 6. Parameters of the asynchronous motor

Rated power	1000 W
Blades	3
Blades diameters	2.26 m
Startup wind speed	3.4 m/s
Rated wind speed	12.5 m/s

NOMENCLATURE

I_m	Maximum current, A	R_s	Statoric resistance, Ω
I_{pv}	Photovoltaic current, A	V_m	Maximum voltage, V
I_{sc}	Short circuit current, A	V_{oc}	Open circuit voltage, V
i_r	Rotor current, A	V_{pv}	Photovoltaic voltage, V
i_s	Stator current, A	MPPT	Maximum Power Point Tracking
L_m	Magnetizing inductance of the IM, H	P&O	Perturbation and Observation
L_r	Rotor inductance of the IM, H	PV	Photovoltaic
L_s	stator inductance of the IM, H	SOC	State of charge of battery
R_r	Rotoric resistance, Ω	SOCmax	State of charge

REFERENCES

- Chouidira I, Khodja D.J, Chakroune S. Fuzzy Logic Based Broken Bar Fault Diagnosis and Behavior Study of Induction Machine. *Journal Européen des Systèmes Automatisés* 2020; 53(2), pp 233-242.
- Gam O, Abdelati R, Tankari M A, Mimouni M F. An improved energy management and control strategy for wind water pumping system. *Transactions of the Institute of Measurement and Control* 2019; 1-15.
- Goppelt F, Hieninger T, Schmidt-Vollus R. Modeling Centrifugal Pump Systems from a System-Theoretical Point of View. 18th International Conference on Mechatronics - Mechatronika (ME) 2018, Brno, Czech Republic.
- Laadissi1 E.M, El Filali A, Zazi M, El Ballouti A. Comparative Study Of Lead Acid Battery Modelling. *ARNP Journal of Engineering and Applied Sciences* 2018; 13(15), pp 4448-4452.
- Obaid W, Hamid A, Ghenai Ch. Solar/wind pumping system with forecasting in Sharjah, United Arab Emirates. *International Journal of Electrical and Computer Engineering (IJECE)* 2021; 11(4), pp 2752-2759.
- Pant S, Saini R.P. Solar Water Pumping System Modelling and Analysis using MATLAB/Simulink. *IEEE Students Conference on Engineering & Systems (SCES)* 2020; Prayagraj, India.
- Perissinotto R M, Monte Verde W, Biazussi J L, Vieira Bulgarelli N A, Denner Pires Fonseca W, Souza de Castro M, Erick de Moraes Franklin, Bannwart A C. Flow visualization in centrifugal pumps: A review of methods and experimental studies. *Journal of Petroleum Science and Engineering* 2021; 203, 108582.
- Poompavai T, Kowsalya M. Control and energy management strategies applied for solar photovoltaic and wind energy fed water pumping system: A review. *Renewable and Sustainable Energy Reviews* 2019; 107, pp 108–122.
- Serir Ch, Rekioua D, Mezzai N, Bacha S. Supervisor control and optimization of multi-sources pumping system with battery storage. *Int J Hydrogen Energy* 2016; 41(45), pp 20974-20986.
- Xiao Xu, Weihao Hu, Di Cao, Qi Huang, Cong Chen, Zhe Chen. Optimized sizing of a standalone PV-wind-hydropower station with pumped-storage installation hybrid energy system. *Renewable Energy* 2020; 147, pp 1418-1431.
- Zaibi M, Cherif H, Champenois G, Sarenib B, Roboamb X, Belhadjc J. Sizing methodology based on design of experiments for freshwater and electricity production from multi-source renewable energy systems. *Desalination* 2018; 446, pp 94-113.